

1

2

3

4

5 **Selfish bacteria are active throughout the water column of the ocean**

6

7

8

9 Greta Giljan¹, Sarah Brown², C. Chad Lloyd³, Sherif Ghobrial³, Rudolf Amann¹, Carol Arnosti³

10

11 1) Department of Molecular Ecology, Max Planck Institute for Marine Microbiology,

12 Bremen, Germany

13 2) Program in Ecology, Energy, and the Environment, University of North Carolina-Chapel

14 Hill, Chapel Hill NC USA

15 3) Department of Marine Sciences, University of North Carolina-Chapel Hill, Chapel Hill NC

16 USA

17

18

19 Heterotrophic bacteria use extracellular enzymes to hydrolyze high molecular weight (HMW)
20 organic matter to low molecular weight (LMW) hydrolysis products that can be taken into the
21 cell. These enzymes represent a considerable investment of carbon, nitrogen, and energy, yet the
22 return on this investment is uncertain, since hydrolysis of a HMW substrate outside a cell yields
23 LMW products that can be lost to diffusion and taken up by scavengers that do not produce
24 extracellular enzymes¹. However, an additional strategy of HMW organic matter utilization,
25 ‘selfish’ uptake², is used for polysaccharide degradation, and has recently been found to be
26 widespread among bacterial communities in surface ocean waters³. During selfish uptake,
27 polysaccharides are bound at the cell surface, initially hydrolyzed, and transported into the
28 periplasmic space without loss of hydrolysis products², thereby retaining hydrolysate for the
29 selfish bacteria and reducing availability of LMW substrates to scavenging bacteria. Here we
30 show that selfish bacteria are common not only in the sunlit upper ocean, where polysaccharides
31 are freshly produced by phytoplankton, but also deeper in the oceanic water column, including in
32 bottom waters at depths of more than 5,500 meters. Thus, the return on investment, and therefore
33 also the supply of suitable polysaccharides, must be sufficient to maintain these organisms.

34

35 High molecular weight carbohydrates – polysaccharides - constitute a major fraction of
36 both living and detrital marine organic matter^{4,5}. The degradation of polysaccharides depends
37 largely on the activities of bacteria equipped with the extracellular enzymes required to
38 dismantle these often highly complex structures to low molecular weight (LMW) pieces (e.g., ⁶).
39 Since LMW hydrolysis products may also be taken up by ‘scavengers’ that do not produce the
40 enzymes, the enzyme ‘producers’ that carry out external hydrolysis might benefit only in part
41 from their own enzyme activities¹. Selfish bacteria circumvent this problem by transporting large

42 polysaccharide fragments into their periplasmic space, minimizing loss of hydrolysis products².
43 A broad range of polysaccharides is taken up via selfish mechanisms by diverse bacteria in
44 surface ocean waters⁷; the speed and extent of selfish uptake and external hydrolysis vary by
45 geographic location^{7,8}, as well as by the nature and abundance of polysaccharides at different
46 phytoplankton bloom stages⁹. The extent to which selfish bacteria are present and active in other
47 depths of the ocean, however, remains unexplored.

48 Given that polysaccharide-hydrolyzing enzymes are exquisitely specific for substrate
49 structure¹⁰, we hypothesized that selfish bacteria would be most abundant and active in locations
50 and depths at which freshly produced – structurally unaltered – polysaccharides are common.
51 Since both HMW dissolved organic matter and particulate organic matter are more abundant and
52 are ‘fresher’ – have a higher fraction of chemically characterizable components – in the upper
53 ocean than in the deep ocean^{11,12}, we expected that selfish bacteria would be particularly
54 dominant in the upper water column. We therefore collected water samples at three stations
55 characterized by different physical, chemical, and productivity conditions in the western North
56 Atlantic: in the Gulf Stream, in productive waters off of the coast of Newfoundland, and in the
57 oligotrophic waters of the North Atlantic Gyre (Fig. S1). At these stations, we collected water
58 from the surface, deep chlorophyll maximum (33 to 104 meters), upper mesopelagic (~300 m),
59 and bottom (3190 to 5580 m). Triplicate incubations were made with water from three different
60 Niskin bottles from each depth (biological replicates). We quantified the presence and activity of
61 selfish bacteria by adding small quantities of structurally-distinct fluorescently-labeled
62 polysaccharides (FLA-PS) and incubating these water samples at *in situ* temperatures. The added
63 FLA-PS – laminarin, pullulan, fucoidan, xylan, chondroitin sulfate, and arabinogalactan – have
64 different monomer compositions and linkage types. These polysaccharides were chosen because

65 they are abundant in marine algae and phytoplankton and/or because a wide range of marine
66 bacteria may produce enzymes that hydrolyze them (e.g., ¹³⁻¹⁶). We concurrently measured
67 selfish uptake and external hydrolysis rates of the FLA-PS, quantified cell abundances, measured
68 bacterial protein production, and tracked bacterial community composition.

69 Much to our surprise, selfish bacteria were abundant at all water depths that we
70 investigated. These bacteria were identified microscopically by the co-localization of the blue
71 DAPI staining of DNA and the associated intense green staining from the FLA-PS (Fig. 1).
72 Considerable selfish activity was evident even at the t0 timepoint, when 14-17% of bacteria in
73 surface water, 5-22% at the DCM, 5-8% at 300 m, and 5-12% of bacteria in bottom water took
74 up one of the FLA-PS (Fig. 2a-d). With increasing incubation time, the proportion of cells taking
75 up one of the FLA-PS increased, especially in sub-surface waters. Selfish uptake reached a
76 maximum of 13-18% of DAPI-stainable cells in surface waters, 14-26% at the DCM, 12-18% at
77 300 m, and 25-67% in bottom water. Uptake at the t0 timepoint reflects the short-term response
78 of the *in situ* community, since the time elapsed between substrate addition and sample
79 processing is likely insufficient for major changes in community composition, while later
80 timepoints reflect the activities of a community that has changed in composition with time.

81 The *in situ* bacterial communities showed considerable selfish uptake, despite initial
82 station- and depth-related differences in composition (Fig. 3). These initial communities changed
83 markedly for the most part over the time course of incubation (Fig. 4; Figs S2-S5), but selfish
84 uptake at most stations and depths remained constant or increased after the t0 timepoint. The
85 compositional changes in unamended incubations were very similar to the incubations amended
86 with FLA-PS, demonstrating that the addition of FLA-PS by themselves had little influence on
87 community composition (Figs. S2c-S5c) or cell counts (Fig. S6). Moreover, the changes in

88 community composition typically were not convergent for different depths (Fig. S7), in that
89 different genera dominated even in cases where similar classes became more abundant with time.
90 For example, although Gammaproteobacteria became relatively more abundant with time in
91 many of the incubations (Fig. 4, Figs. S2-S5), the dominant phylotypes varied by depth and
92 station (Figs. S8-S10); there were no obvious connections between specific changes in bacterial
93 community composition and selfish uptake.

94 Although selfish uptake mechanisms have been studied most intensively in members of
95 the gut-dwelling Bacteroidetes^{17,18}, our previous investigations in surface ocean waters
96 demonstrated that a range of bacteria, including members of the Bacteroidetes, Planctomycetes,
97 Verrucomicrobia, and the genus *Catenovulum* (Gammaproteobacteria) carry out selfish
98 uptake^{7,19}. Furthermore, a large fraction of the selfish population is still unidentified^{7,19}. The
99 observation of selfish activity at multiple depths throughout the water column against a
100 background of changing bacterial community composition suggests that this strategy of substrate
101 acquisition is widespread, and in the ocean is not restricted to a limited range of bacterial taxa.
102 Since selfish uptake cannot be inferred solely from genomic information²⁰, however, we cannot
103 yet determine whether selfish uptake mechanisms are as widely distributed as the ability to
104 produce extracellular enzymes to carry out external hydrolysis.

105 We observed remarkable differences in patterns of selfish uptake and external hydrolysis,
106 which were measured in the same incubations. While selfish uptake was measurable for a broad
107 range of polysaccharides at all stations and all depths, external hydrolysis was more variable
108 among stations at similar depths, and decreased sharply in bottom water compared to surficial
109 waters (Fig. 2). In surface waters at Stn. 19, for example, all polysaccharides except fucoidan
110 were externally hydrolyzed, but at Stns. 18 and 20 only laminarin, chondroitin, and xylan were

111 externally hydrolyzed; these spatial variations in external hydrolysis are consistent with previous
112 observations in surface ocean waters²¹. Station-related variability was also evident at a depth of
113 300 m: at Stns. 18 and 20, a broad spectrum of polysaccharides was hydrolyzed, but at Stn. 19,
114 only xylan, laminarin, and pullulan were hydrolyzed. In bottom waters of all three stations, only
115 two or three polysaccharides were hydrolyzed – laminarin and xylan at Stn. 18, laminarin, xylan,
116 and chondroitin at Stn. 19, and laminarin and chondroitin at Stn. 20 – at comparatively low rates,
117 first evident at late incubation timepoints. Overall, the spectrum of substrates hydrolyzed was
118 narrower and the hydrolysis rates in deep water were considerably lower than in surface water,
119 consistent with the few previous reports of polysaccharide hydrolysis in deep ocean waters²²⁻²⁴.
120 Patterns of external hydrolysis and selfish uptake at the same stations and depths thus showed
121 striking contrasts.

122 The presence of selfish bacteria in the water column, also at depths well below the
123 euphotic zone, requires new consideration of the economics of substrate processing and uptake.
124 Two-player models of enzyme producers and scavengers have considered the conditions under
125 which extracellular enzyme production may pay off (e.g.,¹), such as when polysaccharides are
126 abundant²⁵, or when they are found in sufficiently dense patches²⁶. Inclusion of selfish bacteria in
127 this calculus, as described in a new conceptual model²⁷, suggests that substrate structural
128 complexity, as well as abundance, needs to be taken into account. Selfish uptake, in which
129 hydrolysate is efficiently captured, can help ensure that investment in extracellular enzymes
130 generates sufficient return. From this perspective, selfish uptake appears to be widespread i)
131 when a substrate is highly complex and requires considerable enzymatic investment, or ii) when
132 there is high competition for a very widely-available substrate, such that competition is a primary
133 consideration.

134 The first case covers enzymatic investment to acquire comparatively rare and structurally
135 complex substrates that are selfishly taken up, as in the deep ocean (Fig. 4). Arguably, intact
136 polysaccharides are likely a comparatively rare commodity in most of the subsurface ocean, and
137 thus should be a target for selfish uptake, a consideration that would explain the broad range of
138 substrates selfishly taken up in much of the water column. Polysaccharides such as fucoidan are
139 particularly good examples for a potential pay-off from selfish uptake, since fucoidan hydrolysis
140 requires an extraordinary investment in extracellular enzymes²⁸. Moreover, external hydrolysis
141 of fucoidan is comparatively rarely detected in the surface ocean²¹, and to date has not been
142 detected in deep ocean waters^{29,22-24}. The second set of circumstances for which selfish uptake
143 pays off – high competition for an abundant polysaccharide – applies especially to laminarin.
144 Oceanic production of laminarin has been estimated to be on the order of 12-18 gigatons
145 annually^{13,30}, providing a vast supply of readily-degradable substrate to heterotrophic microbial
146 communities. Moreover, external hydrolysis of laminarin is measurable in almost every site and
147 location in the ocean investigated to date^{21, 27, 22-24, 3, 7-9}, pointing at extraordinarily widespread
148 capabilities to utilize this polysaccharide. Selfish uptake of this polysaccharide therefore ensures
149 return on enzyme investment by capturing a substrate that would otherwise be acquired by
150 competitors.

151 Here we show for the first time that selfish uptake occurs at multiple depths in the water
152 column, including in deep bottom waters. Furthermore, rapid selfish uptake of polysaccharides in
153 bottom water provides important clues about the physiology of bacteria in the deep ocean, as
154 well as the nature of the substrates that they use. Approximately 5-10% of the bacterial
155 community at our three deep ocean sites was ready and able to take up specific polysaccharides
156 shortly after addition (Figs. 1- 2, Fig. 4). This response is notable in light of the observation that

157 uptake of a simple amino acid at these depths (as demonstrated by leucine used for bacterial
158 productivity measurements; Table S1), which does not require prior enzymatic hydrolysis, was
159 quite low especially at Stns. 18 and 19. These observations together suggest that a bacterial
160 strategy focused on rapid uptake of structurally more-complex, higher molecular weight
161 polysaccharides pays off in deep water because there is a sufficient supply of these substrates,
162 whereas the *in situ* inventory of individual amino acids in bottom water is likely too low³¹ to
163 merit special targeting by bacteria. Although we currently lack data on the polysaccharide
164 component of POM in bottom waters, a new method to specifically quantify laminarin in POM
165 has demonstrated a considerable laminarin concentration in POM in the upper water column
166 (including measurements to a depth of 300m³⁰). Moreover, time-variable rapid transport of
167 bacteria/particles to bottom water depths has been demonstrated³²; some of this organic matter
168 reaching these depths evidently is fresh, and has not been thoroughly worked over in the upper
169 ocean; this organic matter could include intact polysaccharides. Recent measurements of DOM
170 in deep ocean waters additionally suggest that high molecular weight polysaccharides are added
171 to the DOM pool circulating in the deep ocean³³.

172 Evidence of selfish uptake of highly complex polysaccharides in the deep ocean supports
173 the point that the flux of relatively unaltered organic matter to the deep ocean must be of
174 sufficient magnitude³⁴⁻³⁵ to support a viable and reactive population of selfish bacteria in the
175 deep. The presence of bacteria that are capable of processing complex substrates in a selfish
176 manner also points out that measurements of bacterial metabolism that are dependent upon
177 uptake of monomeric substances have likely underestimated an important fraction of
178 heterotrophic carbon cycling activity, since the enzymatic systems used for selfish uptake are
179 specifically tuned to their target substrates². The prevalence of selfish uptake against a backdrop

180 of changing bacterial community composition (Fig. 2, Fig. 4, Figs. S2-S5), moreover, suggests
181 that selfish uptake as a substrate acquisition strategy pays off sufficiently that it is comparatively
182 widespread among bacteria. Selfish uptake is important not only in the surface waters of the
183 ocean, but also in the upper mesopelagic and deep ocean, and is carried out by heterotrophic
184 bacteria whose carbon cycling activities help drive much of the marine carbon cycle.

185

186

187 **Methods**

188 **i. Station location and seawater collection**

189 Seawater was collected at three stations in the western North Atlantic aboard the research vessel
190 *Endeavor* (cruise EN638) using a sampling rosette of 30-liter Niskin bottles fitted with a Sea-
191 Bird 32 conductivity-temperature-depth (CTD) profiler, between May 15th and 30th 2019 (Fig.
192 S1). Collection depths included surface water (2.5–6 m water depth), the deep-chlorophyll
193 maximum (DCM; depth identified via chlorophyll fluorescence signal of the CTD: 104 m, 33 m,
194 64 m water depth at Stns. 18, 19, and 20, respectively), ~300 m (300 m at Stns. 18 and 20; 318 m
195 at Stn. 19), and bottom water (3,190 m, 4,325 m, and 5,580 m, at Stns. 18, 19, and 20,
196 respectively; Fig. S1).

197

198 At each station and depth, triplicates of 600 mL (DCM and bottom water) or 290 mL (surface
199 and 300 m water) were added to sterile, acid rinsed (10% HCl) bottles and incubated for up to 30
200 days in the dark at *in situ* temperatures (room temperature (RT) for water from the surface, DCM
201 and 300 m; 4°C for bottom water) with one of the six FLA-PS: arabinogalactan, chondroitin
202 sulfate, fucoidan, laminarin, pullulan and xylan, each at 3.5 µM monomer equivalent

203 concentration. A single live treatment control without the addition of any substrate was included
204 for the DCM and bottom waters; autoclaved killed controls were included for each substrate at
205 each station and each depth, and were incubated under the same conditions alongside
206 polysaccharide incubations

207

208 Subsamples for microbial cell counts and selfish FLA-PS uptake were collected from DCM and
209 bottom water incubations 0, 1, 3, 7, and 10 days after the addition of polysaccharides; in surface
210 and 300 m incubations, subsamples were collected 0, 3, 7, 10, and 15 days after polysaccharide
211 addition. Note also that the t0 timepoint measurements of selfish uptake represent a time period
212 of ca. 30 min (surface, 300m) to 5 hrs (DCM, bottom water), representing the time required after
213 initial substrate addition to go back and process all of the samples to which substrate had been
214 added. To measure the extracellular hydrolysis of FLA-PS, subsamples were collected on days 0,
215 3, 7, 10, 15, and 30 of the incubations. Subsamples for bulk community analysis were taken
216 before the addition of FLA-PS and at day 1, 3, and 10 of the incubation with DCM and bottom
217 water and at day 0, 3, 7, 10, and 15 in the surface and 300 m incubations.

218

219 **ii. Synthesis of FLA-PS and measurements of extracellular enzymatic activities**

220 Arabinogalactan, chondroitin sulfate, fucoidan, laminarin, pullulan, and xylan were fluorescently
221 labeled with fluoresceinamine (Sigma) and characterized according to Arnosti (2003)³⁶.
222 Subsamples (2 ml) were removed at days 0, 1, 3, 7, 10, 15, and 30 days post FLA-PS addition,
223 and analyzed after Arnosti (2003)³⁶. Note that the added substrate is in competition with
224 naturally occurring substrates, and thus calculated hydrolysis rates are potential hydrolysis rates.

225

226 **iii. Counts of total and substrate-stained cells**

227 **Cell counts:**

228 To prepare samples, 25-50 mL of 1% FA fixed sample were filtered onto a 0.22 μm pore size
229 polycarbonate filter at a maximum vacuum of 200 mbar. The DNA of filtered cells was
230 counterstained using 4',6-diamidin-2-phenylindol (DAPI) and mounted with a
231 Citifluor/VectaShield (4:1) solution. A minimum of 45 microscopic images per sample were
232 aquired as described by Bennke *et al.* (2016)³⁷ with a fully automated epifluorescence
233 microscope (Zeiss AxioImager.Z2 microscope stand, Carl Zeiss) equipped with a cooled
234 charged-coupled-device (CCD) camera (AxioCam MRm + Colibri LED light source, Carl Zeiss),
235 three light-emitting diodes (UV-emitting LED, 365 nm for DAPI; blue-emitting LED, 470 nm
236 for FLA-PS 488) and a HE-62 multi filter module with a triple emission filter (425/50 nm,
237 527/54 nm, LP 615 nm, including a triple beam splitter of 395/495/610, Carl Zeiss) using a 63x
238 magnification oil immersion plan apochromatic objective with a numerical aperture of 1.4 (Carl
239 Zeiss). Final cell enumeration on the acquired images was performed using the image analysis
240 software ACMETOOL (<http://www.technobiology.ch> and Max Planck Institute for Marine
241 Microbiology, Bremen). Automated cell counts were checked manually.

242

243 Total microbial cell numbers and FLA-PS stained cells were counted in a single experimental
244 setup, following Reintjes *et al.* (2017)³. Counting validation was done through manual cell
245 counting on all stains. Selfish substrate uptake could be measured for only four or five of the six
246 polysaccharides used; at all stations and depths, xylan incubations yielded high background
247 fluorescence, which interfered with cell counting; this problem also affected efforts to count cells
248 for pullulan uptake in surface waters and at a depth of 300 m. Note also that we report the

249 fraction of cells carrying out selfish uptake under the assumption that each substrate is taken up
250 by different bacteria (i.e., when reporting that for example 22% of total DAPI-stainable cells
251 were substrate-stained, we add together the percentages taking up laminarin, fucoidan,
252 arabinogalactan, and chondroitin). Since selfish uptake of each substrate is measured in different
253 incubations (triplicate incubations of each individual substrate), however, it is possible that some
254 or all of the cells taking up one substrate also take up another substrate via a selfish mechanism.

255

256 **iv. Super-resolution imaging of selfish polysaccharide uptake**

257 The specific substrate accumulation pattern in FLA-PS stained cells was visualized on a Zeiss
258 LSM780 with Airyscan (Carl Zeiss) using a 405 nm, a 488 nm, and a 561 nm laser with
259 detection windows of 420-480 nm, 500-550 nm, and LP 605 nm, respectively. Z-stack images of
260 the cells were taken with a Plan-Apochromat 63x/1.4 oil objective and the ZEN software
261 package (Carl Zeiss) was used for subsequent AiryScan analysis.

262

263 **v. Taxonomic bacterial community analysis**

264 The initial bacterial communities and their change over the course of the incubation were
265 determined through bulk 16S rRNA analysis. Therefore, 25 mL samples from each incubation
266 were filtered onto a 0.22 μ m pore size polycarbonate filter at a maximum vacuum of 200 mbar,
267 dried and frozen at -20 °C until further processing. Total DNA extraction from filter was done
268 using the DNeasy Power Water Kit (Quiagen). Determination of the concentration as well as the
269 size of the extracted DNA was done via gel chromatography using a Fragment AnalyzerTM
270 (Advanced Analytical). Amplification of the variable 16S rRNA regions V3 and V4 (490 bp)
271 was done in 30 cycles using the 5 PRIME HotMasterMix (Quantabio) together with the

272 Bakt_314F (CCTACGGGNGGCWGCAG) and Bakt_805R
273 (GACTACGVGGGTATCTAATCC)³⁸ PCR primer pair with an individual 8 bp barcode adapter
274 (based on the NEB Multiplex Oligos for Illumina, New England Biolabs) attached to the forward
275 primer and the reverse primer. The amplified PCR product was purified and size selected using
276 the AMPure XP PCR Cleanup system (Beckman Coulter). Barcoded products were pooled in
277 equimolar concentrations and send for paired-end Illumina sequencing (2x250 bp HiSeq2500) to
278 the Max Planck-Genome-center Cologne. Sequences were merged, demultiplexed and quality
279 trimmed (sequence length 300–500 bp, < 2% homopolymers, < 2 % ambiguities) with
280 BBTools³⁹. The SILVAngs pipeline⁴⁰ with the SSU rRNA SILVA database 138 was used for
281 sequence comparison and taxonomic assignment of the retrieved sequences.

282

283 **vi. Statistical analysis of bacterial communities**

284 Analysis of the bacterial community composition was done normalized reads representing >
285 1,000 reads per sample and the average of triplicates for the FLA-PS amended incubations was
286 used for further analysis and visualization. Archaeal and eukaryal reads were excluded from
287 analysis. Differences in the community composition between station, water depth, incubation
288 time, and substrate amended to unamended incubations were analyzed by analysis of similarity
289 (ANOSIM) and visualized in non-metric multi-dimensional scaling (NMDS) plots, using Bray-
290 Curtis dissimilarity matrices. The community shift over the course of the incubation was
291 visualized by the comparison of the read abundance on genus level from the initial community to
292 the respective read abundance in the incubations over time.

293

294 **vii. Bacterial productivity**

295 Bacterial productivity was measured after Kirchman et al. (2001)⁴¹. In brief, bacterial protein
296 production was calculated from leucine incorporation rates, measured in samples that were
297 incubated at *in-situ* temperatures in the dark for time periods of 12 to 24 h. Bacterial carbon
298 production was calculated by multiplying bacterial protein production by 0.86^{42,41}.

299

300 **viii. Data availability**

301 Bacterial 16S rRNA gene sequences were archived as Illumina-generated libraries at the
302 European Nucleotide Archive (ENA) of The European Bioinformatics Institute (EMBL-EBI)
303 under the accession number PRJEB45894.

304

305 **Acknowledgments**

306 We thank the captain and crew of R/V *Endeavor*, as well as the other members of the scientific
307 party of the EN638 cruise, for excellent work at sea. Andreas Ellrot (MPI Bremen) provided
308 essential support for the microscopic analyses. This project was funded by NSF OCE- 1736772
309 to CA, with additional funding by the Max Planck Society.

310

311 **Author contributions**

312 Conceived and planned project: CA, RA. Carried out work at sea: GG, SB, CCL, SG, RA, CA.
313 Analyzed samples post-cruise: GG, SB, CCL, SG. Created figures: GG, SB. Wrote manuscript:
314 GG, SB, CA with input from all co-authors.

315

316

317 **References**

318

319 1. Allison, S.D. Cheaters, diffusion and nutrients constrain decomposition by microbial enzymes in
320 spatially structured environments. *Ecol. Lett.* **8**, 626–635 (2005).

321

322 2. Cuskin, F. *et al.* Human gut Bacteroidetes can utilize yeast mannan through a selfish mechanism.
323 *Nature* **517**, 165–173 (2015).

324

325 3. Reintjes, G., Arnosti, C., Fuchs, B. M. and Amann R. An alternative polysaccharide uptake
326 mechanism of marine bacteria. *ISME J.* **11**, 1640–1650 (2017).

327

328 4. Biersmith, A. & Benner, R. Carbohydrates in phytoplankton and freshly produced dissolved
329 organic matter. *Mar. Chem.* **63**, 131–44 (1998).

330

331 5. Hedges, J. I. *et al.* The biochemical and elemental compositions of marine plankton: a NMR
332 perspective. *Mar. Chem.* **78**, 47–63 (2002).

333

334 6. Hehemann, J.-H. *et al.* Biochemical and structural characterization of the complex agarolytic
335 enzyme system from the marine bacterium *Zobellia galactanivorans*. *J. Biol. Chem.* **287**, 30571–
336 30584 (2012).

337

338 7. Reintjes, G., Arnosti, C., Fuchs, B. M. & Amann, R. Selfish, sharing, and scavenging
339 bacteria in the Atlantic Ocean: a biogeographic study of microbial substrate utilisation. *ISME*
340 *J.* **13**, 1119–1132 (2019).

341

342 8. Reintjes, G., Fuchs, B. M., Amann, R. & Arnosti, C. Extensive microbial processing of
343 polysaccharides in the South Pacific Gyre via selfish uptake and extracellular hydrolysis. *Front.*
344 *Microbiol.* **11**, 3242 (2020a).

345

346 9. Reintjes, G. *et al.* Short-term changes in polysaccharide utilization mechanisms of marine
347 bacterioplankton during a spring phytoplankton bloom. *Environ. Microbiol.* **22**, 1884–1900
348 (2020b).

349

350 10. Lombard, V., Golaconda Ramulu, H., Drula, E., Coutinho, P. M. & Henrissat, B. The
351 carbohydrate-active enzymes database (CAZy) in 2013. *Nuc. Acids Res.* **42**, 490–495 (2014).

352

353 11. Wakeham, S. G., Lee, C., Hedges, J. I., Hernes, P. J. & Peterson, M.L. Molecular indicators of
354 diagenetic status in marine organic matter. *Geochim. Cosmochim. Acta* **61**, 5363–5369 (1997).

355

356 12. Benner, R. & Amon, R. M. W. The size-reactivity continuum of major bioelements in the ocean.
357 *Ann. Rev. Mar. Sci.* **7**, 185–205 (2015).

358

359 13. Alderkamp, A. C., Van Rijssel, M. & Bolhuis, H. Characterization of marine bacteria and the
360 activity of their enzyme systems involved in degradation of the algal storage glucan laminarin. *FEMS*
361 *Microbiol. Ecol.* **59**, 108–117 (2007).

362

363 14. Haug, A. & Myklestad, S. Polysaccharides of marine diatoms with special reference to
364 *Chaetoceros* species. *Mar. Biol.* **34**, 217–222 (1976).

365

366 15. Wegner, C. E. *et al.* Expression of sulfatases in *Rhodopirellula baltica* and the diversity of
367 sulfatases in the genus *Rhodopirellula*. *Mar. Genom.* **9**, 51–61 (2013).

368

369 16. Xing, P. *et al.* Niches of two polysaccharide-degrading Polaribacter isolates from the North
370 Sea during a spring diatom bloom. *ISME J.* **9**, 1410–1422 (2015).

371

372 17. Koropatkin, N. M., Cameron, E. A. & Martens, E. C. How glycan metabolism shapes the human gut
373 microbiota. *Nat. Rev. Microbiol.* **10**, 323–335 (2012).

374

375 18. Rakoff-Nahoum, S., Foster, K. R. & Comstock, L. E. The evolution of cooperation within the gut
376 microbiota. *Nature* **533**, 255–259 (2016).

377

378 19. Giljan, G., Arnosti, C., Amann, R. & Fuchs, B. M. Seasonal changes in bacterial
379 polysaccharide utilization off Helgoland. Preprint at <http://> (2021).

380

381 20. Klassen, L. *et al.* Quantifying fluorescent glycan uptake to elucidate strain-level variability in
382 foraging behaviors of gut bacteria. *Microbiome* **9**, 1-18 (2021).

383

384 21. Arnosti, C., Steen, A. D., Ziervogel, K., Ghobrial, S. & Jeffrey, W. H. Latitudinal gradients
385 in degradation of marine dissolved organic carbon. *PLoS ONE* **6**, e28900 (2011).

386

387 22. Hoarfrost, A. & Arnosti, C. Heterotrophic extracellular enzymatic activities in the Atlantic
388 Ocean follow patterns across spatial and depth regimes. *Front. Mar. Sci.* **4**, 200 (2017).

389

390 23. Balmonte, J. P., Teske, A. & Arnosti C. Structure and function of high Arctic pelagic,
391 particle-associated, and benthic bacterial communities. *Environ. Microbiol.* **20**, 2941-2954
392 (2018).

393

394 24. Balmonte J. P., Simon, M., Ansgar-Giebel, H. & Arnosti, C. A Sea Change in microbial
395 enzymes: Heterogeneous latitudinal and depth-related gradients in bulk water and particle-
396 associated enzymatic activities from 30°S to 59°N in the Pacific Ocean. in press, *Limnol.*
397 *Oceangr.* (2021).

398

399 25. Traving, S. J., Thygesen, U. H., Riemann, L. & Stedmon, C. A. A model of extracellular
400 enzymes in free-living microbes: which strategy pays off? *Appl. Environ. Microb.* **81**, 7385-7393
401 (2015).

402

403 26. Ebrahimi, A., Schwartzman, J. & Cordero, O. X. Cooperation and spatial self-organization
404 determine rate and efficiency of particulate organic matter degradation in marine bacteria. *PNAS*
405 **116**, 23309–23316 (2019).

406

407 27. Arnosti, C. *et al.* The biogeochemistry of marine polysaccharides: sources, inventories, and
408 bacterial drivers of the carbohydrate cycle. *Ann. Review of Marine Science* **13**, 81-108 (2021).

409

410 28. Sichert, A. *et al.* Verrucomicrobia use hundreds of enzymes to digest the algal polysaccharide
411 fucoidan. *Nat. Microbiol.* **5**, 1026-1039 (2020).

412

413 29. Steen, A. D, Zervogel, K., Ghobrial, S. & Arnosti, C. Functional variation among
414 polysaccharide-hydrolyzing microbial communities in the Gulf of Mexico. *Mar. Chem.* **138**, 13–
415 20 (2012).

416

417 30. Becker, S. *et al.* Laminarin is a major molecule in the marine carbon cycle. *PNAS* **117**, 6599-6607
418 (2020).

419

420 31. Giljan, G. *et al.* Bacterioplankton reveal years-long retention of Atlantic deep-ocean water by the
421 Tropic Seamount. *Sci. Rep.* **10**, 1-11 (2020).

422

423 32. Poff, K. E., Leu, A. O., Eppley, J. M., Karl, D. M. & Delong, E. F. Microbial dynamics of elevated
424 carbon flux in the open ocean's abyss. *PNAS* **118**, e2018269118 (2021).

425

426 33. Broek, T. A. B. *et al.* Low molecular weight dissolved organic carbon: aging, compositional
427 changes, and selective utilization during global ocean circulation. *Global Biogeochem. Cycles* **34**,
428 e2020GB006547 (2020).

429

430 34. Hansell, D. A., Carlson, C. A., Repeta, D. J. & Schlitzer, R. Dissolved organic matter in the ocean.
431 *Oceanography* **22**, 202–211 (2015).

432

433 35. Bergauer, K. *et al.* Organic matter processing by microbial communities throughout the Atlantic
434 water column as revealed by metaproteomics. *PNAS* **115**, 400-408 (2018).

435

436 36. Arnosti, C. Fluorescent derivatization of polysaccharides and carbohydrate-containing
437 biopolymers for measurement of enzyme activities in complex media. *J. Chromat. B* **793**, 181–
438 191 (2003).

439

440 37. Bennke, C. M. *et al.* Modification of a high-throughput automatic microbial cell enumeration
441 system for shipboard analyses. *Appl. Environ. Microbiol.* **82**, 3289-3296 (2016).

442

443 38. Herlemann, D. P. R. *et al.* Transitions in bacterial communities along the 2000 km salinity
444 gradient of the Baltic Sea. *ISME J.* **5**, 1571–1579 (2011).

445

446 39. Bushnell, B. BBTools software package. URL <http://sourceforge.net/projects/bbmap> 578
447 (2014).

448

449 40. Quast, C. *et al.* The SILVA ribosomal RNA gene database project: improved data processing
450 and web-based tools. *Nuc. Acids Res.* **41**, 590–596 (2013).

451

452 41. Kirchman, D. L. Measuring bacterial biomass production and growth rates from leucine
453 incorporation in natural aquatic environments. *Methods in Microbiol.* **30**, 227–238 (2001).

454

455 42. Simon, M. & Azam, F. Protein content and protein synthesis rate of planktonic marine bacteria. *Mar.*
456 *Ecol. Prog. Ser.* **51**, 201–213 (1989).

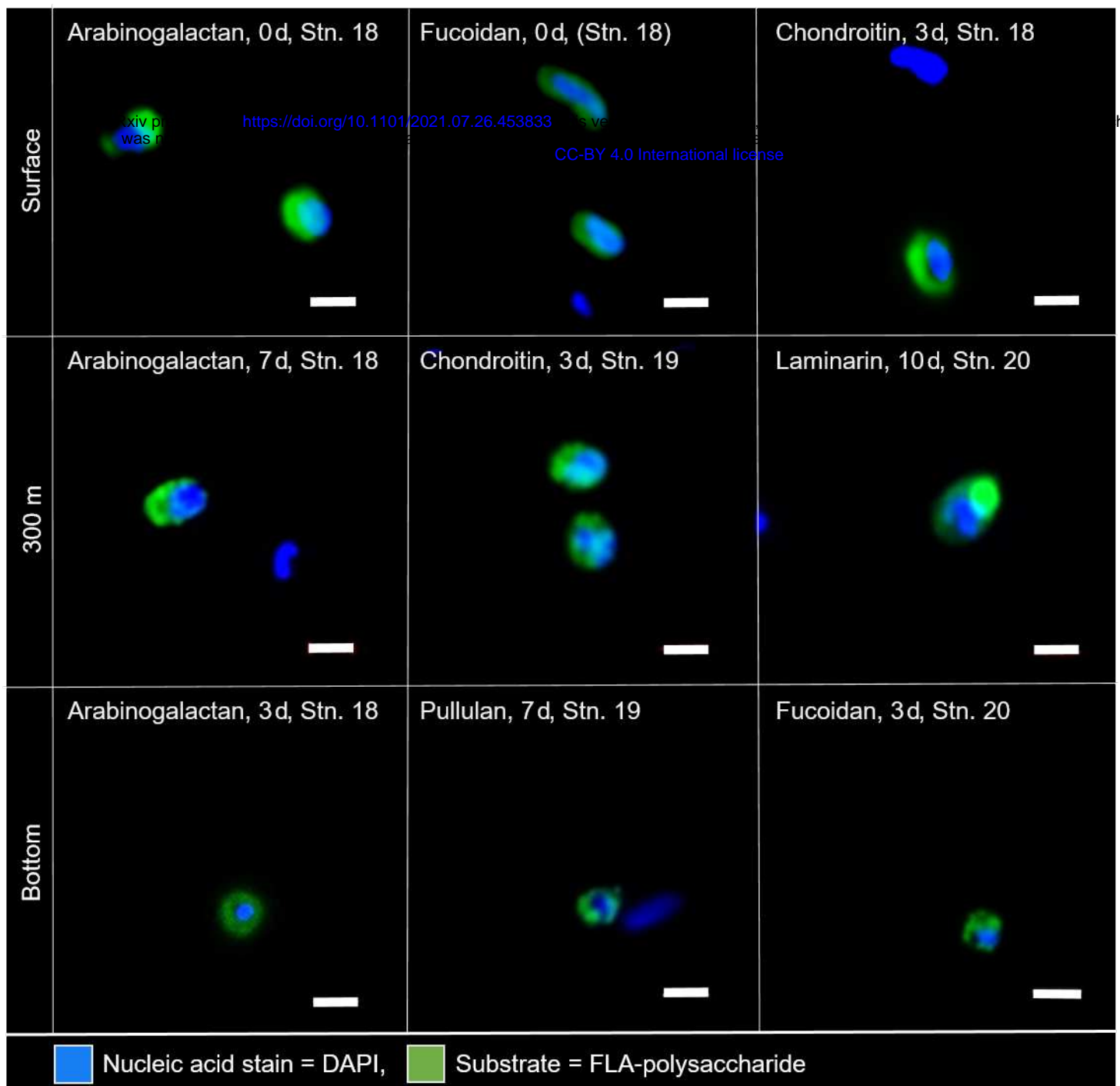


Figure 1 Selfish bacteria throughout the water column in the western North Atlantic Ocean. Super-resolution images of microbial cells from surface water, 300 m water depth, and bottom water (3,190 m, 4,325 m, and 5,580 m, respectively) showing accumulation of fluorescently labeled arabinogalactan, fucoidan, chondroitin sulfate, laminarin, and pullulan due to selfish uptake. Blue signal (DAPI) shows nucleic acids, green signal is due to fluoresceinamine-labeled polysaccharides. Scale bar = 1 μ m.

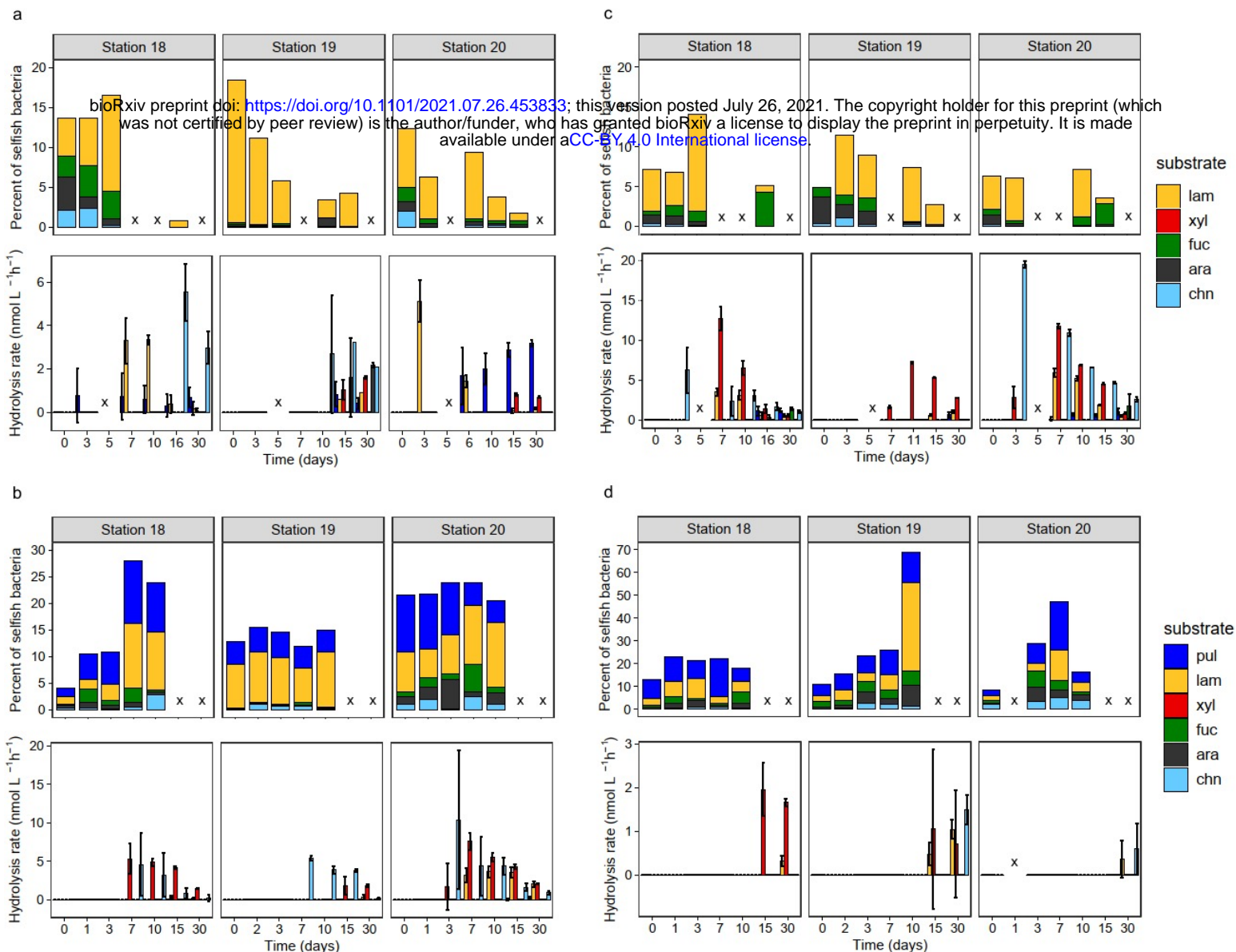
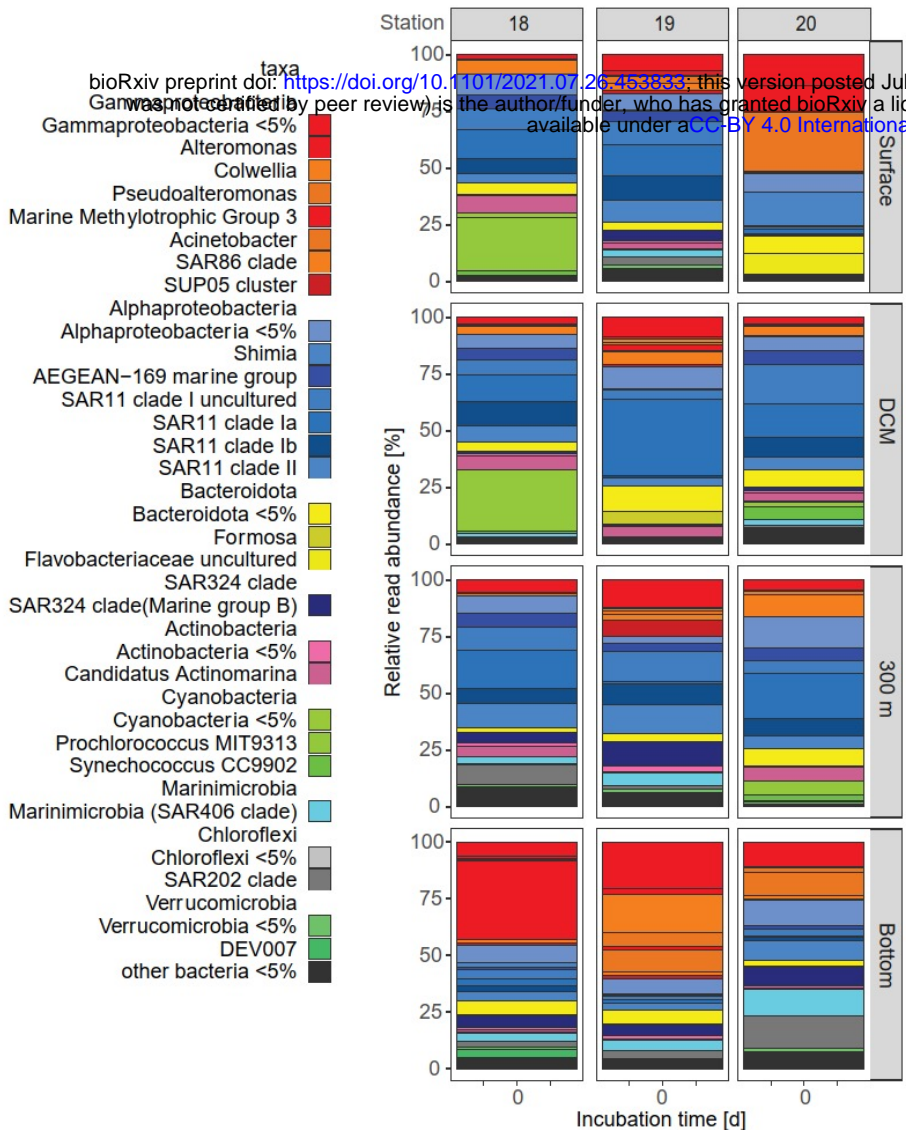
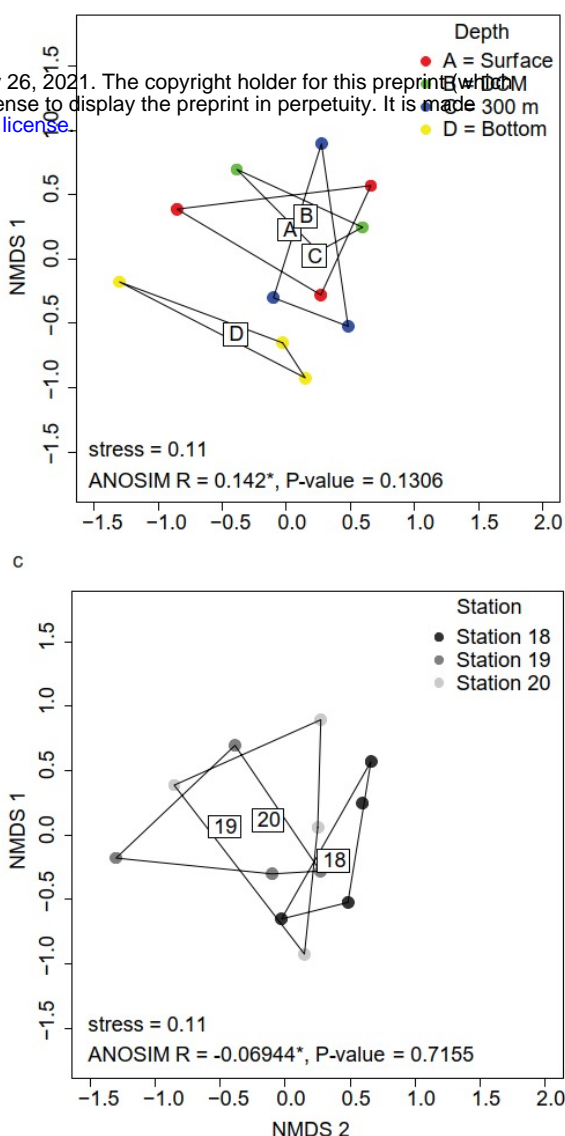


Figure 2 Heterotrophic polysaccharide utilization throughout the water column at three distinct locations in the western North Atlantic Ocean. Selfish uptake and extracellular (external) hydrolysis of six different fluorescently labeled polysaccharides (FLA-PS) in **(a)** surface waters, **(b)** at the DCM, **(c)** at 300 m water depth, and **(d)** in bottom waters at Stations 18, 19 and 20 over the course of individual FLA-PS amended incubations. Note that selfish FLA-xylan uptake at all stations and FLA-pullulan uptake in surface waters and at 300 m depth could not be analyzed due to high background fluorescence and are therefore not included in the data. Error bars represent the average of biological replicates ($n = 3$). Samples marked with an 'x' were not analyzed.

a



b



c

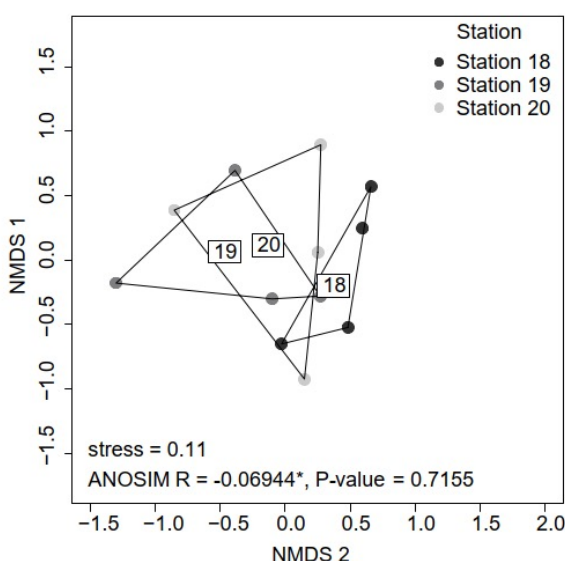


Figure 3 The initial bacterial communities at four depths at three distinct locations in the western North Atlantic. Bacterial communities (a) differ more by (b) depth but are also different by (c) station. * denotes statistically significant results. Each community represents the average of biological replicates ($n = 3$).

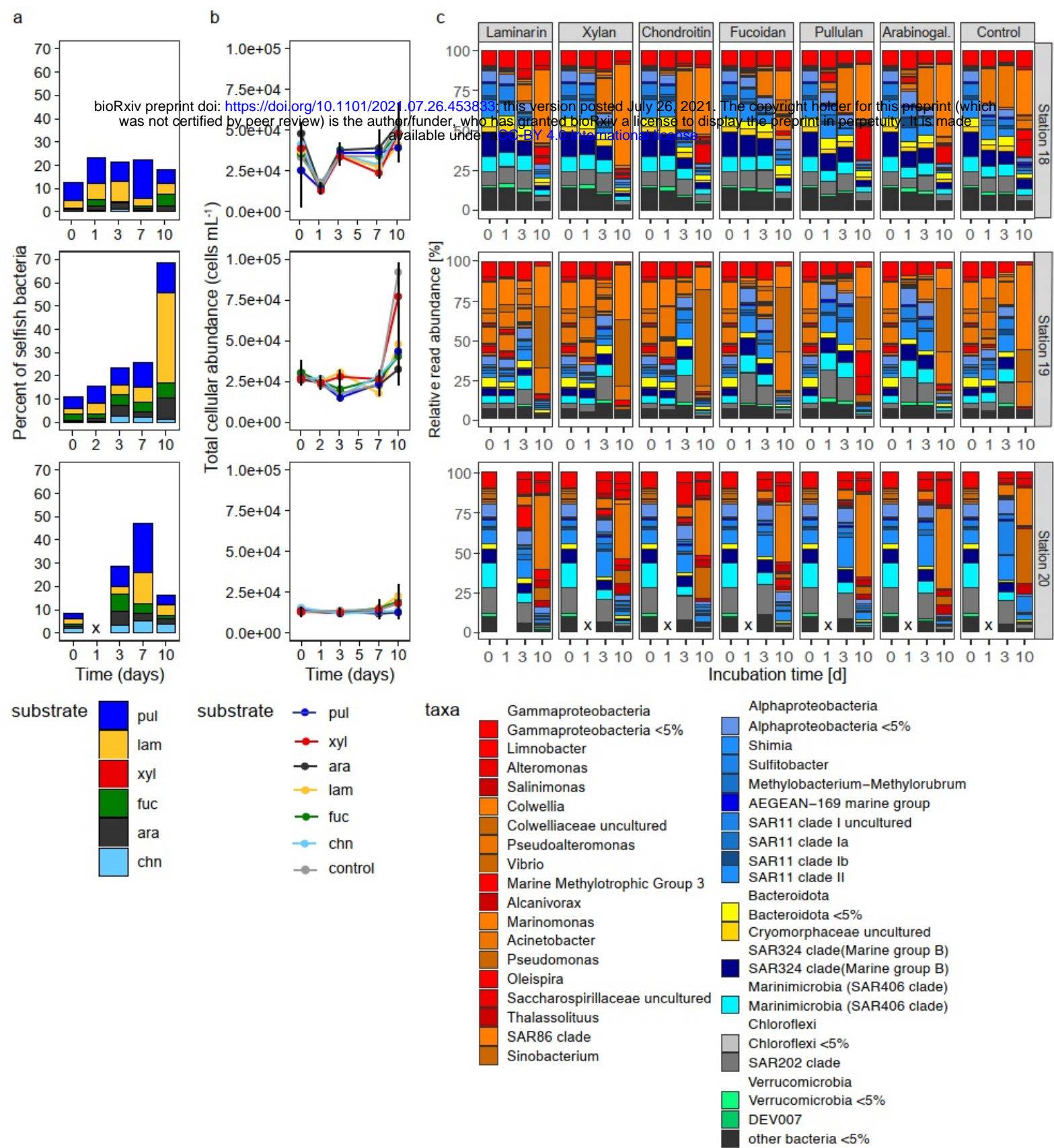


Figure 4 Selfish polysaccharide uptake, cell counts, and bacterial community composition in North Atlantic bottom water. **(a)** Selfish uptake of FLA-PS over the course of 10 day FLA-PS amended incubations at Stations 18, 19 and 20 (same data as in Fig. 2d). **(b)** Development of the total microbial cell counts and **(c)** bacterial community composition in each of the FLA-PS amended incubations from (a), and in the unamended treatment control. The initial community shortly after the addition of the FLA-PS is depicted at 0 days of incubation. Bars represent the average of up to 3 replicates. Time points marked with an x were not analyzed.